CEAS-GNC-2022-042

CEAS EuroGNC 2022
"Conference on Guidance, Navigation and Control"
3-5 May 2022 @ Technische Universität Berlin, Germany

Impact Time Control with Bézier Curves

Suwon Lee Assistant Professor, Department of Future Mobility, Kookmin University, 02707, 77 Jeongneung-ro, Seongbuk-gu, Seoul, Republic of Korea. suwon.lee@kookmin.ac.kr

Raziye Tekin Senior Lead Engineer, Roketsan, 06780, Elmadag Ankara, Turkey. razytekin@gmail.com

ABSTRACT

An optimal impact time control guidance algorithm is presented. The optimal trajectory of the missile in planar engagement geometry is obtained using optimal output trajectory shaping technique. For the practical usefulness, the condition for bounded acceleration is derived in which the lateral acceleration command not to grow unbounded near the final time. Optimal trajectories for different objective functions are investigated, and the obtained optimal trajectories are compared.

Keywords: Impact time control guidance, Missile systems, Trajectory optimization, optimal guidance

1 Introduction

The fundamental objective of the missile guidance is that it must lead the pursuer to the target. In addition to this, the application of interest might necessitate other objectives such as impact time. Impact time is mainly required when there is operational time constraint; for instance, controlling each missile's time of impact, where all can be the same value or sequential regardless of their initial positions. Another application of impact time control is synchronizing the impact time of the salvo attack members, which mostly requires a communication in between the missiles and/or control unit of the attack [1]-[4]. Nevertheless, it is possible to have a salvo attack scenario with all the impact time control guidance laws within the common impact time interval, which may vary depending on the method.

One of the earliest works of impact time control guidance law bases on proportional navigation (PN) guidance law with a bias term, which is the difference between the desired and the estimated time-to-go with PN for the linear kinematics [5]. In [6], the authors extended their method in [5] by enhancing the time-to-go estimation for the nonlinear kinematics, where the final guidance law turns into a biased PN and the impact time error as the bias. [7] is also a biased PN for impact time control, where the PN is denoted as the nominal feedback command based on Lyapunov stability theory and the bias related with the time-to-go estimation for every PN guidance gain greater than one and for wide heading errors. [8] presents a different methodology such that it does not need time-to-go estimation but instead forces the trajectory to follow a look angle profile, where the guidance law turns out to be a switched PN structure. Apart from PN based methods Lyapunov theory and sliding mode control methods are also used to design impact time control [9]-[11]. [9] implements the time-to-go estimation given in [5] and [10] on the other hand prefers the time-to-go estimation given in [1].

Apart for the methods which based on the time-to-go estimation and PN guidance law, recently several geometrical methodologies have been developed [11]-[15]. In [11], impact time control problem is solved in a closed loop fashion for any order for time dependent polynomial of look angle including the minimum effort impact time control solution for the linearized kinematics. In [12], look angle is desired to be a circular arc and the guidance law is derived under this geometry, where approximate closed-form solutions are obtained in [12]. In [13], trajectory is shaped to be a circular one with the exact time-to-go since the trajectory itself is predefined. [14] designs the range as a function of time and then the time of impact is demanded from such a profile, where the effectiveness of the closed loop guidance is also shown under disturbances. In addition to such shaping methods, [15] provides an impact time control guidance law based on elliptic trajectory in addition to polynomials and circular ones with the distinction of using three-point guidance. [16] and [17] are the two recent examples of Bézier functions used for trajectory shaping algorithms. In [16], Bézier function is used to estimate spacecraft trajectories to fit a set of measured positions. [17] provides solution for impact time and the angle, where the state and the input trajectories are represented as parametric functions.

In this study, the impact time control with Bézier curves is proposed. By optimizing the shape of the geometric curve, the optimal trajectory of the states of the nonlinear missile engagement system is attained as representing the state trajectory with the curve. Exploiting the structure of the nonlinear missile engagement system with relative degree two, the trajectories of the states including the relative distance and look angle are represented as a parametric function of time. An important difference between the proposed method and existing methods is the fact that the proposed method does not require linearized kinematics and the shape of the trajectory can be optimized for an arbitrary cost function as required.

In Section 2, preliminaries are presented including the engagement geometry and shaping of the trajectory with respect to time. Afterwards, the boundary conditions are defined. The optimization problem formulation based on output trajectory shaping technique is delivered in Section 3. The results are presented in Section 4. Finally, Section 5 concludes this study.

2 Preliminaries

2.1 Missile Engagement Geometry

The nonlinear missile geometry is described in Fig. 1 where R is relative distance from missile to the target, V is a constant speed of the missile, σ, γ, and λ are look angle, flight path angle, and line-of-sight angle, respectively. The nonlinear dynamic equations of motion are defined as follows.

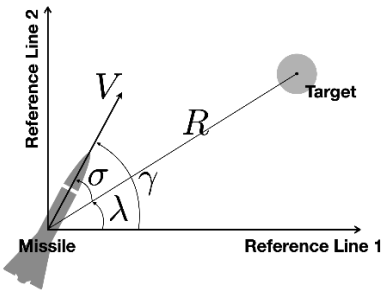

Fig. 1 Engagement geometry

$$\dot{R}(t) = -V\cos\sigma(t) \tag{1}$$

$$\dot{\sigma}(t) = \frac{V\sin\sigma(t)}{R(t)} + \dot{\gamma}(t) \tag{2}$$

$$\dot{\lambda}(t) = \dot{\gamma}(t) - \dot{\sigma}(t) \tag{3}$$

Note that the missile engagement geometry can be defined as a nonlinear system with states $\mathrm{x}(t) = [R(t), \sigma(t)\,]^T$ and control input $u(t) = \dot{\gamma}(t)$. When we choose the system output as $y(t) = R(t)$, the system's relative degree becomes 2.

2.2 Conditions for Bounded Accelerations

Differentiating the system output $y(t) = R(t)$ with respect to time *t* is written as follows:

$$\ddot{R}(t) = V\sin\sigma(t)\,\dot{\sigma}(t) = \frac{V^2}{R(t)}(\sin\sigma(t))^2 + V\sin\sigma(t)\,\dot{\gamma}(t) \tag{4}$$

From (1), $\left(\dot{R}/V\right)^2 = (\cos\sigma)^2 = 1 - (\sin\sigma)^2$ and

$$\begin{aligned}\ddot{R} &= \frac{V^2}{R}\left(1 - \frac{\dot{R}^2}{V^2}\right) \pm V\dot{\gamma}\sqrt{1 - \frac{\dot{R}^2}{V^2}} \\ &= \frac{1}{R}\left(V^2 - \dot{R}^2\right) \pm \dot{\gamma}\sqrt{V^2 - \dot{R}^2}\end{aligned} \tag{5}$$

where $\left\|\dot{R}/V\right\| \leq 1$. Rearranging the equation with respect to the control input $\dot{\gamma}$ gives,

$$\pm\dot{\gamma} = \frac{\ddot{R}}{\sqrt{V^2 - \dot{R}^2}} - \frac{\sqrt{V^2 - \dot{R}^2}}{R} \tag{6}$$

From (6), it can be noticed that as $R(t) \to 0, \dot{R}^2(t) \to V^2$, the magnitude of $\dot{\gamma}(t)$ blows up. The following assumption validates (6) for all $t \in [0, t_f]$.

Assumption 1.

We assume that $V^2 - \dot{R}(t)^2 \neq 0$ and $R(t) > 0$ for $t \in [0, t_f]$.

Because the objective of the missile is to successfully intercept the target, the range to the target at the final time should be a very small value but not zero considering Assumption 1. The boundary condition is written as follows.

$$0 < R(t_f) = \varepsilon_1 \ll 1 \tag{7}$$

In order not to make the second term in (6) blow up, let us consider the following condition.

$$0 < \sqrt{V^2 - \dot{R}^2(t_f)} = \varepsilon_2 \leq \varepsilon_1 \ll 1 \tag{8}$$

In similar, for the first term in (6),

$$0 < \left|\ddot{R}(t_f)\right| = \varepsilon_3 \leq \varepsilon_2 \leq \varepsilon_1 \ll 1 \tag{9}$$

Therefore, the control $\dot{\gamma}(t_f)$ at the final time becomes as follows

$$\dot{\gamma}(t_f) = \pm\frac{\varepsilon_3}{\varepsilon_2} - \frac{\varepsilon_2}{\varepsilon_1} \tag{10}$$

Because that the magnitude of the two terms in (10) are both equal to or smaller than 1, the control $\dot{\gamma}(t_f)$ does not blow up.

The parameters $\varepsilon_1, \varepsilon_2$, and ε_3 are design parameters that a user can specify. Hence, the control at the final time can be chosen. In this study, for a practical issue, the optimal parameters that minimizes the control at the final time is selected. When ε_1 and ε_3 are given, consider the following cost function.

$$J(\varepsilon_2) = \left(\frac{\varepsilon_3}{\varepsilon_2} - \frac{\varepsilon_2}{\varepsilon_1}\right)^2 \tag{11}$$

Differentiating $J(\varepsilon_2)$,

$$\frac{dJ}{d\varepsilon_2}(\varepsilon_2^*) = 2\left(\frac{\varepsilon_3}{\varepsilon_2^*} - \frac{\varepsilon_2^*}{\varepsilon_1}\right)\left(-\frac{\varepsilon_3}{\varepsilon_2^*} - \frac{1}{\varepsilon_1}\right) \equiv 0$$
$$\varepsilon_2^* = \sqrt{\varepsilon_1\varepsilon_3} \tag{12}$$

where ε_2^* is the optimal parameter that minimizes the control at the final time. Substituting ε_2^* into (10) gives,

$$\dot{\gamma}(t_f) = 0 \text{ or } -2\sqrt{\frac{\varepsilon_3}{\varepsilon_1}} \tag{13}$$

Note that $\ddot{R}(t_f)$ should be a positive value to make the control at the final time zero.

3 Optimal Guidance Algorithm

3.1 Dynamic Optimization Problem Formulation

Here, the dynamic optimization problem is formulated. For the optimal guidance, various structures of cost function can be considered. An energy minimizing optimal guidance problem is a common example:

$$C = \int_{t_0}^{t_f} \dot{\gamma}(t)^2 dt \tag{14}$$

The dynamic constraints are (**1-3**), and the boundary conditions for state variables are given as follows.

$$R(0) = R_0, \;\; R(t_f) = R_f = \varepsilon_1$$
$$\sigma(0) = \sigma_0, \;\; \sigma(t_f) = \sigma_f \tag{15}$$

In this study, rather dealing with the optimization problem directly using conventional dynamic optimization technique, the optimal output trajectory shaping using Bézier curve from [17] is used. Because the boundary condition at final time is represented with respect to the time differentiations of $R(t)$, it is convenient to apply the optimal output trajectory shaping algorithm.

3.2 Optimal Output Trajectory Shaping

Using the optimal output trajectory shaping using Bézier curve, the output trajectory is represented with Bézier curve as follows:

$$y(t) = \mathbf{B}_N(\tau) = \sum_{v=0}^{N} b_{v,N}(\tau)\mathbf{P}_v\,, \quad \tau \in [0,1] \tag{16}$$

$$b_{v,N}(\tau) = \binom{N}{v}\tau^v(1-\tau)^{N-v} \tag{17}$$

where $\mathbf{B}_N(\tau)$ is the Bézier curve of degree N, $\mathbf{P}_v$ is the control point of Bézier curve τ is the curve parameter, and $\binom{N}{v}$ is the binomial coefficients defined as:

$$\binom{N}{v} = \frac{N!}{v!\,(N-v)!} \tag{18}$$

By the linear parameterization between t and τ,

$$\tau = \frac{t}{t_f} = \mu t \tag{19}$$

The output trajectory $y(t) = R(t)$ is represented with polynomial of time. Because the relative degree of the system and the number of states are the same, every state of the system can be represented as parametric function[17].

In the optimal output trajectory shaping algorithm, the control points of Bézier curve are optimized to find optimal trajectory. Some of the control points are determined by the boundary conditions. Also note that the final time t_f can be specified by selecting proper μ that one can obtain impact time control trajectory of the missile.

In this study, the boundary conditions at the initial time are considered as follows.

$$\begin{aligned} y(0) &= R_0 = \mathbf{B}_N(0) \\ \dot{y}(0) &= -V\cos\sigma_0 = \mu\mathbf{B}_N{}'(0) \end{aligned} \tag{20}$$

Where $(\cdot)'$ stands for the differentiation with respect to τ. The control points of $\mathbf{B}_N(\tau)$ are determined by (20) as follows.

$$\begin{aligned} \mathbf{P}_0 &= R_0 \\ \mathbf{P}_1 &= \mathbf{P}_0 - \frac{V\cos\sigma_0}{N} \end{aligned} \tag{21}$$

In similar, the control points at the final time are determined as follows.

$$\begin{aligned} \mathbf{P}_N &= \varepsilon_1 \\ \mathbf{P}_{N-1} &= \mathbf{P}_N - \frac{\sqrt{V^2 - \varepsilon_2^2}}{\mu N} \\ \mathbf{P}_{N-2} &= -\mathbf{P}_N + 2\mathbf{P}_{N-1} + \frac{\varepsilon_3}{\mu^2 N(N-1)} \end{aligned} \tag{22}$$

Note that Bézier curve with $N \geq 5$ is required to satisfy boundary conditions. Therefore, to secure the degree of freedom to optimize the curve shape, $N > 6$ is required. The positions of the free control points affect the shape of the curve and one can obtain optimal curve by optimizing the positions of the free control points.

4 Numerical Examples

The optimal impact time control guidance trajectories are investigated. In this study, the optimization cost functions are designed as follows. First, the total control effort is considered, then the maximum acceleration and the maximum look angle are considered, which are the important physical constraints of the physical systems. Afterwards, the trajectory obtained from optimal output trajectory shaping algorithm is compared with the trajectory from optimal guidance algorithm, which minimizes the total control effort, i.e., $\int a^2 dt$ is numerically solved via MATLAB® function bvp4c, where the coding details is given in [19].

$$C_1 = \frac{1}{t_f - t_0}\int_{t_0}^{t_f} \dot{\gamma}(t)^2 dt \tag{23a}$$

$$C_2 = \max|\dot{\gamma}(t)| \tag{23b}$$

$$C_3 = \max|\sigma(t)| \tag{23c}$$

$R_0 = 5{,}000\text{m}$, $\sigma_0 = 1e^{-4}$, $V = 200\,\text{m/s}$, $\varepsilon_1 = 0.3$, $\varepsilon_3 = 1e^{-5}$ are used. The desired impact time is 35 s. Note that σ_0 is not zero because when it is zero, (**6**) becomes invalid. ε_2 is determined from (12). The optimal trajectories and the time histories for different cost functions are depicted in Fig. 2 and Fig. 3, where it is seen that the boundary conditions are satisfied. The control input $\dot{\gamma}$ at the initial and time of impact changes very sharply, because of the numeric nonzero $\ddot{R}(t)$ value the initial and final time.

The result of the first solution is $0.010435(\text{rad}^2/\text{s}^3)$ and the second one is $0.009926\ (\text{rad}^2/\text{s}^3)$. Note that although the curve with $N = 7$ has only one degree of freedom, the cost function value from output trajectory shaping algorithm is close to the value from optimal guidance. Also, the shapes of the trajectories are similar with that of the optimal guidance. For example, $\dot{\gamma}(t_f)$ smoothly converges to zero, which could be desired for practical applications as described in [14].

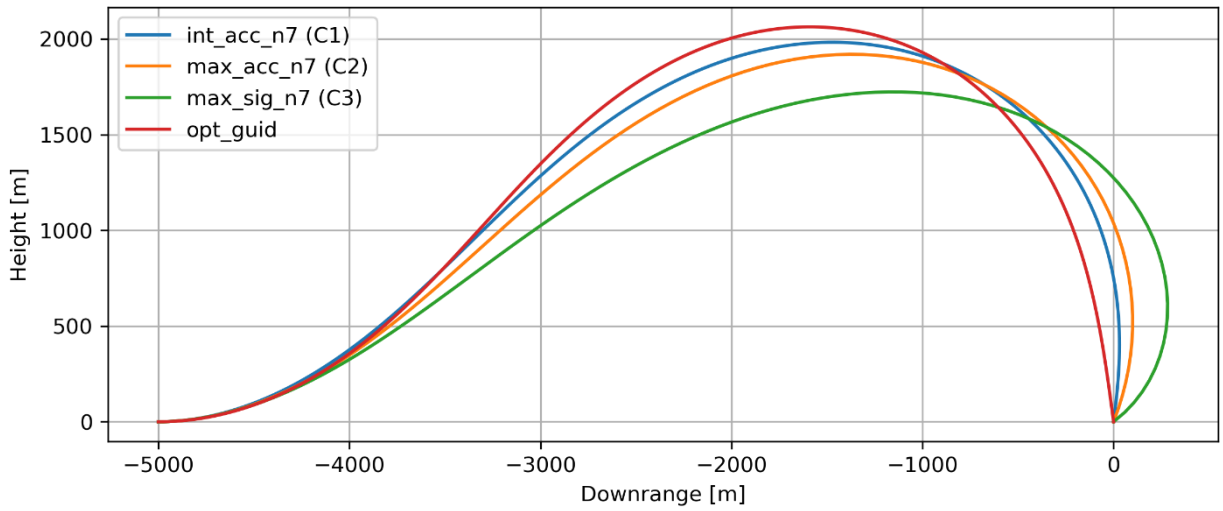

Fig. 2 Trajectories for different cost function

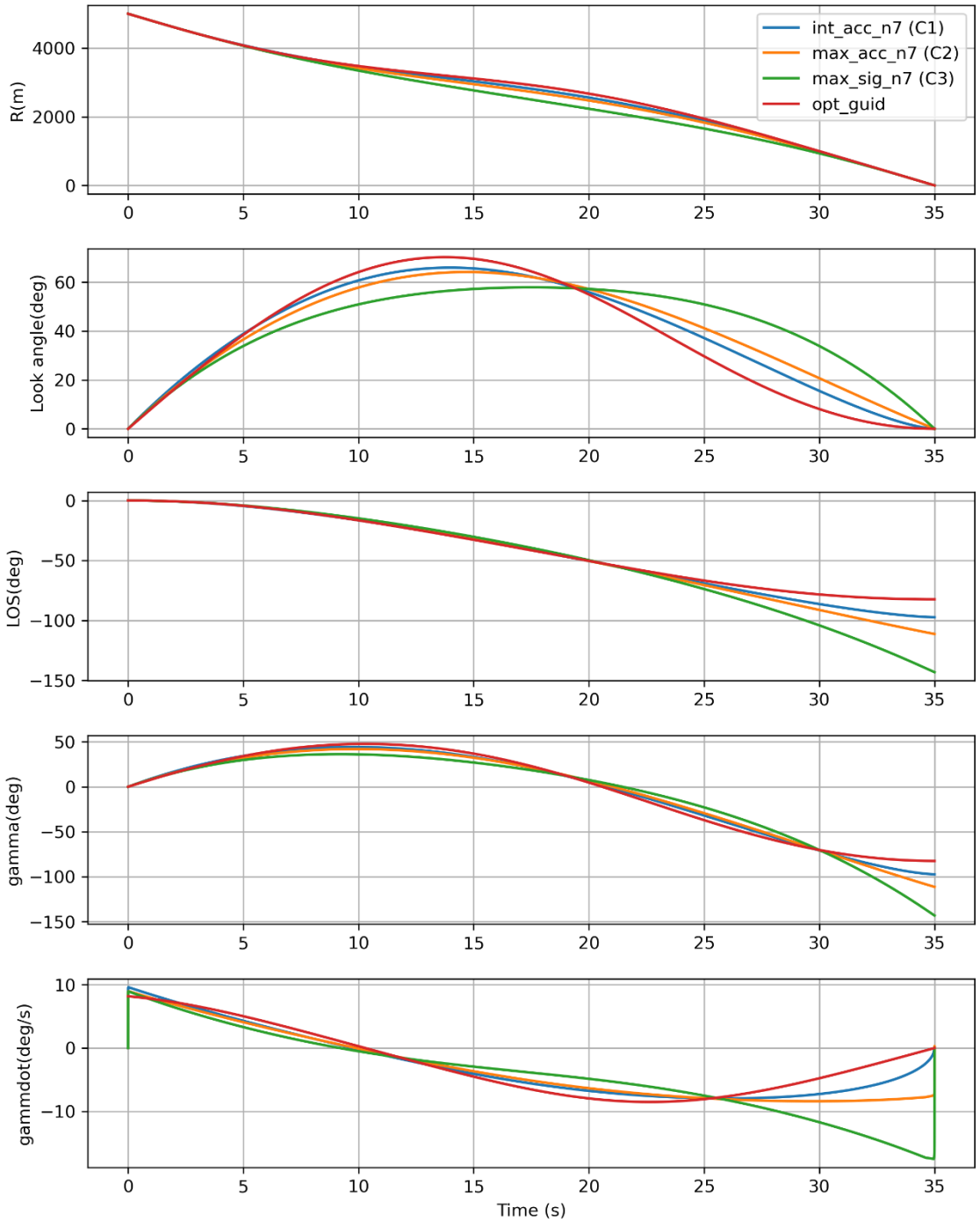

Fig. 3 Simulation results of the engagement

The trajectory from optimal guidance algorithm is also depicted Fig. 2. The blue line (proposed trajectory shaping algorithm) and the red line (energy optimal guidance algorithm) shares the same cost function. Note that although the curve with $N = 7$ has only one degree of freedom, the cost function value from output trajectory shaping algorithm is close to the value from optimal guidance. Also, the shapes of the trajectories are similar with that of the optimal guidance.

The cost function values for different trajectories are summarized in Table 1. The trajectory from energy optimal guidance has the best cost function value for C1 and C2, which is expected because the energy optimal guidance is designed to minimize the cost function numerically throughout the trajectory,

while the trajectory created by the output shaping algorithm has limitation such that the trajectory is an approximated optimal trajectory. The cost function values increasing degree *N* are given in Table 2. Note that trajectories with higher *N* show lower C1 values. It can be understood that increasing *N* gives more degree of freedom (more free control points) for the trajectory and therefore the optimization solver could find better solution in the higher dimension.

Because the optimization cost function is highly nonlinear with respect to the optimization parameters, i.e., control points, the numerical solver may find a local minimum solution. In general, it is very important to select the initial points carefully when dealing with the numerical optimization problems to avoid local minima. In this study, the initial control points for degree *N* are selected from the curve of degree *N*-1. This is possible because the Bézier curve of degree *N* can represent every curve that Bézier curve of degree *N*-1 can represent [18].

Table 1 Cost function values for different trajectories

Trajectories (col) / Cost value (row)	C1	C2	C3	Optimal guidance
C1	**0.010435**	0.011626	0.017614	**0.009926**
C2	0.167412	**0.156422**	0.305620	**0.148610**
C3	1.151473	1.120330	**1.010831**	1.226572

Table 2 Cost function values increasing degree *N*

Trajectories	***N***=8	***N***=9	***N***=10	***N***=11	Optimal guidance
C1	0.010251	0.010248	0.010208	0.010164	0.009926

5 Conclusions

In this study, an optimal impact time control guidance algorithm is developed. The trajectory of the relative distance from the missile to the target is parameterized using polynomial curve and represented as a function of time. The Bézier curve is used to represent the trajectory of the relative distance to the target and the shape of the curve is optimized with respect to given cost functions. By selecting a linear parameterization between the time and the curve parameter, the final time of the trajectory can be specified that the impact time control guidance can be attained. The nonlinear engagement geometry between the missile and the target is considered that the states and control input of the nonlinear system are also represented as functions of time. During the optimization process, the nonlinear path constraints are also considered. The numerical optimization result shows that by increasing the polynomial degree of the curve, the optimality can be increased. The obtained optimal trajectory is compared with the trajectory of the optimal guidance algorithm.

References

[1] Jeon, I.-S., Lee, J.-I., and Tahk, M.-J., "Homing Guidance Law for Cooperative Attack of Multiple Missiles," Journal of Guidance, Control, and Dynamics, Vol. 33, No. 1, 2010, pp. 275–280.

[2] Shiyu, Z., and Rui, Z., “Cooperative Guidance for Multi-missile Salvo Attack,” Chinese Journal of Aeronautics, Vol. 21, No. 6, 2008, pp. 533–539.

[3] He, S., Wang, W., Lin, D., and Lei, H., “Consensus-Based Two-Stage Salvo Attack Guidance,” IEEE Transactions on Aerospace and Electronic Systems, Vol. 54, No. 3, 2018, pp. 1555–1566.

[4] Zadka, B., Tripathy, T., Tsalik R., and Shima, T., "A Max-Consensus Cyclic Pursuit Based Guidance Law for Simultaneous Target Interception," *2020 European Control Conference (ECC)*, 2020, pp. 662-667.

[5] Jeon, I.-S., Lee, J.-I., and Tahk, M.-J., “Impact-Time-Control Guidance Law for Anti-Ship Missiles,” IEEE Transactions on Control Systems Technology, Vol. 14, No. 2, 2006, pp. 260–266.

[6] Jeon, I.-S., Lee, J.-I., and Tahk, M.-J., “Impact-Time-Control Guidance with Generalized Proportional Navigation Based on Nonlinear Formulation,” Journal of Guidance, Control, and Dynamics, Vol. 39, No. 8, 2016, pp. 1187–1892.

[7] Cho, N., and Kim, Y., “Modified Pure Proportional Navigation Guidance Law for Impact Time Control,” Journal of Guidance, Control, and Dynamics, Vol. 39, No. 6, 2016, pp. 852–872.

[8] Tekin, R., Erer, K. S., and Holzapfel, F., “Control of Impact Time with Increased Robustness via Feedback Linearization,” Journal of Guidance, Control, and Dynamics, Vol. 39, No. 7, 2016, pp. 1678 –1684.

[9] Kim, M., Jung, B., Han, B., Lee, S., and Kim, Y., “Lyapunov-Based Impact Time Control Guidance Laws Against Stationary Targets,” IEEE Transactions on Aerospace and Electronic Systems, Vol. 51, No. 2, 2015, pp. 1111–1122.

[10] Cho, D., Kim, H. J, and Tahk, M.-J., “Nonsingular Sliding Mode Guidance for Impact Time Control,” Journal of Guidance, Control, and Dynamics, Vol. 39, No. 1, 2016, pp. 61–68.

[11] Tekin, R., Erer, K. S., and Holzapfel, F., “Adaptive Impact Time Control Via Look-Angle Shaping Under Varying Velocity,” Journal of Guidance, Control, and Dynamics, Vol. 40, No. 12, 2017, pp. 3247–3255.

[12] Wang, P., Guo, Y., and Ma, G., “New Differential Geometric Guidance Strategies for Impact-Time Control Problem,” Journal of Guidance, Control, and Dynamics, Vol. 42, No. 9, 2019, pp. 1982–1992.

[13] Tsalik, R., and Shima, T., “Circular Impact Time Guidance,” Journal of Guidance, Control, and Dynamics, Vol. 42, No. 18, 2019, pp. 1836–1847.

[14] Tekin, R., Erer, K. S., and Holzapfel, F., “Impact Time Control with Generalized-Polynomial Range Formulation,” Journal of Guidance, Control, and Dynamics, Vol. 41, No. 5, 2018, pp. 1190–1195.

[15] Tsalik, R., and Shima, T., “Elliptic Guidance,” Journal of Guidance, Control, and Dynamics Vol. 41, No. 11, 2018, pp. 2435–2444.

[16] de Dilectis, F., Mortari, D., and Zanetti, R., “Bézier Description of Space Trajectories,” Journal of Guidance, Control, and Dynamics, Vol. 39, No. 11, 2016, pp. 2535–2539.

[17] Lee S., and Kim, Y., “Optimal Output Trajectory Shaping Using Bézier Curves,” Journal of Guidance, Control, and Dynamics, Vol. 44, No. 5, pp. 1027-1035, 2021.

[18] Farouki, R. T., and Rajan, V.T., “Algorithms for polynomials in Bernstein form,” Computer Aided Geometric Design, Vol. 5, No. 1, 1988, pp. 1–26.

[19] Erer, K.S., Biased Proportional Navigation Guidance for Impact Angle Control with Extension to Three-Dimensional Engagements,” Ph.D. dissertation, Mechanical Engineering Department, Middle East Technical University, Ankara, Turkey, 2015.